REDVET - Revista electrónica de Veterinaria - ISSN 1695-7504
Vol 25, No. 1 (2024)
http://www.veterinaria.org
Article Received: 5th May 2024, Revised: 10th June 2024, Accepted: 4th July 2024

In Vivo, In Vitro Rt-Pcr Based Gene Expression Studies On Biological Activities Of Biosynthesized Silver Nanoparticles From Tinospora Cordifolia (Thunb.) Plant Extract Against Vibriosis Infection In The Shrimp Litopenaeus vannamei (Boone, 1931)

Ankesh Yadav[1*], Ragunathan M.G[2], Jayanthi.J[3]

[1*,2,3]Department of Advanced Zoology and Biotechnology, Guru Nanak College, Chennai- 600042, Tamil Nadu, India.

ABSTRACT
MDR or multi-drug resistance resulting from the treatment of diseases in shrimp culture is one of the primary difficulties confronting the shrimp business. Shrimp are one of the most popular seafood commodities sold globally worldwide, with aquaculture accounting for the bulk of output. While there are a number of hazardous microbes known to exist in shrimp farming, vibrio strains in particular are a major cause of acute hepatopancreatic necrosis disease (AHPND), which causes severe production losses in the widely farmed white leg shrimp (*Litopenaeus vannamei*). Antimicrobial resistance is spreading across the globe, making disease control critical. It has been shown that medicinal plants have high concentrations of antimicrobial compounds. This work assessed the antibacterial and antioxidant properties of silver nanoparticles synthesized from a plant extract called *Tinospora cordifolia*. An investigation on RT-PCR gene expression was conducted. The purpose of the study is to assess the antibacterial properties of plant *Tinospora cordifolia* against vibriosis infection in shrimp.

Keywords: Antibacterial activity, RT-PCR, SEM, silver nanoparticles, XRD, shrimp.

1. INTRODUCTION

Aquaculture is the globe's fastest-growing food production approach, expanding at a pace of 8% per year. Of the total 167.2 million metric tons of fish in the globe, it makes up 44.1% (FAO, 2016). According to the (FAO, 2020), shrimp is among the most popular seafood dishes, and aquaculture is the fastest-growing food industry worldwide. *Litopenaeus vannamei*, and *Penaeus monodon*, or black tiger prawns, are the two most common types of shrimp farmed. With 5 billion tons generated in 2018, *L.vannamei* is ranked as the sixth most farmed species in the world . West Bengal, Gujarat, Odisha and Tamil Nadu are the primary states in India that engage in shrimp production. The establishment of shrimp farms in India started in the late 1980s as a response to the rising interest from international markets. Approximately 20% of India's 1.2 million hectares of coastal area impacted by salt was utilized for brackishwater aquaculture.This resulted in a seafood value of approximately 24426.74 crores, which accounts for 6.62% of the global production (MPEDA, 2016). Over 90% of the globe's seafood production is produced by Asian aquaculturists, and the industry is still expanding rapidly in developing nations. Especially remarkable is the fact that low-income food-deficit countries (LIFDCs) contribute 82% of the the globe's aquaculture revenue (Dar, 1999).

In recent years, shrimp aquaculture has grown at an unprecedented rate; in fact, over 80,000 hectares of land in coastal India are now dedicated to the practice. However, the most pressing issue confronting the aquaculture industry on a global scale is the prevalence of diseases caused by different types of bacteria, most notably vibrio, which have been detected in shrimp culture systems. *V.harveyi, Pseudomonas spp*. and *Aeromonas spp*. are the most major bacterial pathogens that cause illnesses in shrimp (Teng *et al*., 2017 ; Tacon, 2020).

Vibriosis is a persistent hazard in shrimp farming and is a significant disease issue that causes shrimp mortality globally (Soto *et al*., 2010 ; Babu et al., 2021). *Vibrio harveyi* and *V. parahaemolyticus* are notable infections linked to vibriosis in shrimp among the recognized Vibrio species (Dhar *et al*., 2019). *Vibrio harveyi* is a prominent shrimp disease that may lead to widespread death of penaeid shrimp in hatcheries (de la Pe˜na *et al*., 2001). Numerous Vibrio species may be found in cultured facilities all around the world. Although epizootics often occur in pond-raised shrimp species, illnesses associated to vibrio bacteria typically occur in hatcheries. Gram-negative bacteria belonging to the Vibrionaceae family cause vibriosis. Shrimp suffering with vibriosis have had a variety of issues, including stunted development and infrequent, ultimately mass deaths at various phases of the life cycle (Soto-Rodriguez *et al*., 2010). *Penaeus monodon* hatcheries have 80–100% mortality because to *V.harveyi* luminous strains (Iswarya *et al*., 2022). Shrimp larvae afflicted with vibriosis exhibit impaired sensation, an empty stomach, chromatophores enlarging, and necrosis of appendages. When *V.alginolyticus* or *V. parahaemolyticus* are diagnosed, the cumulative fatalities may be quite high, up to 80% in a matter of days (Li *et al*., 2017). One ongoing problem in shrimp farming has been recognized as vibriosis. As a result of certain *V.harveyi* strains' multiple resistance to streptomycin, cotrimoxazole, and erythromycin which causes mass death in shrimp larvae and progresses to MDR (multi drug resistance), appropriate

REDVET - Revista electrónica de Veterinaria - ISSN 1695-7504
Vol 25, No. 1 (2024)
http://www.veterinaria.org
Article Received: 5th May 2024, Revised: 10th June 2024, Accepted: 4th July 2024

antimicrobial treatment is needed to boost shrimp immunity in order to combat vibriosis infection (Thornber *et al*., 2020).

Antibiotic-resistant infections in farmed species may arise as a result of the usage of antibiotics in aquaculture. Antibiotics are widely recognized to be utilized in shrimp farming as a preventative or therapeutic measure. It is generally known that resistant infections may develop in aquaculture settings (Sørum, 1999; Inglis, 2000), and recent research (Rhodes *et al*., 2000) has shown evidence of plasmids that encode resistance being transferred from aquaculture settings to people. Multi-drug resistance, or MDR, emerges as a worldwide concern. It can be the result of using antimicrobial drugs often or indiscriminately without understanding their pharmacological characteristics. However, using synthetic drugs to treat illnesses comes with a greater expense. Consequently, novel strategies for combating infections are required to battle microbial diseases (Wagner, 1999). It has been shown that medicinal plants contain large amounts of antibacterial chemicals, and there is a growing need for more and more medications made from plant sources. This research examined the antibacterial qualities of *Tinospora cordifolia*, also known as Gulancha in Bengali, a glabrous, succulent climbing shrub native to India, in relation to vibriosis in shrimp (Uddin *et al*., 2010).

Extracts from Tinospora cordifolia are used extensively in conventional medicine and are said to have immune-modulation and adaptogenic properties that help fight infections (Namrta *et al.*, 2013 ; Saxena and Rawat, 2019). Indian medicine is renowned for extending life and strengthening the body's defenses against illness (Ahmadi *et al*., 2023). It has antibacterial properties against many microbial strains due to the presence of phytochemical components such as terpenoids, alkaloids, and steroids (Modi *et al*., 2021). Tinospora cordifolia is an important Indian drug that can be used as a potent agent to tackle vibriosis infection in shrimp.

2. MATERIALS AND METHODS

2.1 *Tinospora cordifolia*

Tinospora cordifolia (Tamil name- Seenthil kodi) (heart-leaved moonseed), was collected from Indian coast guard complex Meenambakkam, Chennai, Tamil Nadu, India. It's a big, leafy climbing vine that spreads widely and has many long, tangled branches and exstipulate leaves with lengthy up to 15 cm petioles (Sharma *et al*., 2019 ; Sinha *et al.*, 2004). After being shade-dried for 20 days, *T. cordifolia* was ground into a powder and kept in an airtight container for later use.

2.2 Preparation of plant extract

A gram of methanol extract was dissolved in 100 milliliters of Milli-Q water and allowed to boil for fifteen minutes. Whatman No. 1 filter paper was used to filter the extract once it had cooled to room temperature. For later usage, the extract was kept at 4 degrees (Pirtarighat *et al*., 2019).

2.3 Biosynthesis of Silver nanoparticles

A 10 mM silver nitrate aqueous solution was made, and it was combined one at a time with fresh methanol extract in a 9:1 ratio. For three hours, this solution was kept at room temperature (30 ± 2°C) on a shaker that was constantly rotating. Indicating the reduction of Ag ions to silver nanoparticles, the mixture's hue shifted from bright green to dark brown (Yu *et al.,* 2019).

2.4 Characterization

Silver nanoparticle was synthesized from Methanol solution of plant extract using silver nitrate solution the synthesized nanoparticles was Confirmed using tool UV, FTIR for chemical compound identification and morphological identification of size and shape of the nanoparticle using SEM, XRD, TEM.

The production of nanoparticles from the precursor metal salt solutions with methanol extract was verified by UV-Vis spectroscopy. With pure water serving as a blank, the absorbing spectrum of the dispersion sample was measured using a UV–Vis spectrometer Shimadzu-UV 1800, covering the wavelength range of 250–800 nm. Fourier-transform infrared spectroscopy (FTIR) study was done to categorize the biomolecules in methanol extract that were liable for reducing metals and stabilizing nanoparticles. X-ray diffraction (XRD) investigation was performed by XPERT-PRO employing monochromatic Cu ka radiation at 40 kV and 30 mA at a 2h angle pattern. The scans ranged from 208 to 808. The silver nanoparticles' morphology and form were analyzed by the utilization of an FEI Quanta 200 FEG MKII scanning electron microscopy (SEM) (FEI, USA). TEM observations were performed using the HITACHI H-800. For setting up the TEM grid, one drop of the bio-reduced dilute solution was placed on a copper grid covered with carbon and allowed to dry under light.

2.5 ANTIOXIDANT ASSAY

2.5.1 Free radical scavenging ability by the use of a stable ABTS radical cation 2,2'-azinobis-(3-ethylbenzothiazoline-6-sulfonic acid)

The ABTS radical cation decolorization assay was used to evaluate the materials' ability to scavenge free radicals (Re *et al.,* 1999). Water was used to dissolve ABTS to a level of 7 mM. By mixing ABTS base solution with 2.45 mM

REDVET - Revista electrónica de Veterinaria - ISSN 1695-7504
Vol 25, No. 1 (2024)
http://www.veterinaria.org
Article Received: 5th May 2024, Revised: 10th June 2024, Accepted: 4th July 2024

potassium persulphate and letting the resultant mixture stand in a dark room temp for 12–16 hours before to use, ABTS radical cation (ABTS*+) was created. When the free radical was kept at ambient temperature in the dark, it remained stable for almost two days. The ABTS*+ solution was diluted with 100% ethanol to an absorbance of 0.700 (±0.02) at 734 nm and allowed to equilibrate at 30°C before the test samples were examined. Reagent blank reading was taken (A_0). After addition of 2.0 mL of diluted ABTS*+ solution, the absorbance reading was taken at 30°C exactly 6 min after initial mixing (A_t). There were three or more attempts made at each determination. The absorbance drop between A_0 and A_t was used to compute the % inhibition of absorbance at 734 nm using the calculation above (Re *et al.,* 1999).
$PI = [(A_{C(0)} - A_{A(t)}) / A_{C(0)}] \times 100$
where $A_{C(0)}$ = control absorbance at t=0 min; and $A_{A(t)}$I = antioxidanat bsorbance at t = 6 min.

2.5.2 DPPH assay (1,1-diphenyl-2-picrilhydrazyl)
The method outlined by Von Gadow *et al*., (1997) was used to evaluate the influence of the samples on the DPPH radical. 50 µl of test sample was mixed with two milliliters of a 6×10^{-5} M DPPH solution. Using a spectrophotometer, the absorbance at 515 nm was constantly monitored for 16 minutes at room temperature.. The percentage of the sample's capacity to scavenge DPPH radicals was determined by plotting the scavenging effect (reduction in absorbance at 515 nm) versus time and using the absorbance value at the conclusion of the 16-minute time frame.Every determination was made three times. Using Yen and Duh's, (1994) method, the samples' % inhibition of the DPPH radical was determined.
$IP = [(A_{C(0)} - A_{A(t)} / A_{C(0)})] \times 100$
where $A_{C(0)}$ = control absorbance at t = 0 min; and $A_{A(t)}$I = antioxidant bsorbance at t = 16 min.

2.5.3 FRAP (Ferric reducing antioxidant power) Assay
The FRAP test was carried out in accordance with Benzie and Strain (1996). Before utilizing, the freshly made working solution was heated to 37 °C by combining 25 mL of acetate buffer, 2.5 mL of TPTZ solution, and 2.5 mL of $FeCl_3$ $6H_2O$ solution. For 30 minutes in the dark, 150 milliliters of the test sample and 2850 ml of the FRAP solution were allowed to react. The colorful result, ferrous tripyridyltriazine complex, was then measured at 593 nm. The percentage of inhibition per milligram of extract is used to express the results.

2.5.4 Nitric oxide scavenging assay
By using the Griess reaction, nitric oxide produced from sodium nitroprusside in an aqueous solution at physiological pH was quantified (Marcocci *et al*., 1994). The test extract (10, 25, 50, and 100 µg/ml) and the reaction mixture (3 ml) including sodium nitroprusside (10 mm) in phosphate buffer saline was incubated at 25ºC for 150 min, 1.5 milliliters of the reaction mixture were withdrawn after incubation, and 1.5 milliliters of Griess reagent were added. At 546 nm, the chromophore's absorbance was measured. The percentage of nitric oxide scavenging inhibition was computed.

2.6 IN VITRO ANTIBACTERIAL ACTIVITY
2.6.1 Test Strains
The test bacterial strains *Pseudomonas aeruginosa*, *Salmonella typhi Staphylococcus aureus* , and *Vibrio harveyi* were obtained from Microbial Type Culture Collection and Genbank (IMTECH, Chandigarh, India).

2.6.2 Antibacterial activity
Well diffusion techniques were used to measure the antimicrobial activity (Holder and Boyce 1994). A sterile Petri plate was filled with around 25 mL of melted Mueller Hinton agar. After allowing the plates to set, the bacteria were distributed across the surface using a sterilized cotton swab applicator to create a culture lawn. A sterilized cork-borer was used to create a 6 mm well on the agar after the microorganisms had been allowed to set for five minutes. The samples for testing were placed into wells at various levels, such as 25 mg/mL, 50 mg/mL, 75 mg/mL, and 100 mg/mL, after being dispersed in sterile water.. The plates were then incubated for twenty-four hours at 37°C in a bacteriological incubator. The diameter of the zone of inhibition was used to calculate the antibacterial activity.

2.7 IN VIVO STUDY
2.8. LC50 (Experimental animals)
Determination of LC50 of SiNPs against shrimps (Gulec *et al*., 2013). Commonly collected or farmed for food, whiteleg shrimp (litopenaeus vannamei), usually referred to as king prawn or Pacific white shrimp, are a species found in the eastern Pacific Ocean. It was collected from a shrimp aquaculture farm in Ponneri, district Thiruvallur, Tamil Nadu, India. *Litopenaeus vannamei* with an average weight of 4-5 g and lengths of 8-9 cm were used in this study. Shrimps were acclimated for 1 week in these aquariums. After this, 5 shrimps were transferred to 10 L aquariums.

2.8.1 Experimental Design
In all, seventy-five shrimp were employed in the experiment. The shrimp were split up into five groups of fifteen fish apiece, with three duplicates of each group (five fish total): Group 1 (control group; non-SiNPs normal shrimp) was fed

REDVET - Revista electrónica de Veterinaria - ISSN 1695-7504
Vol 25, No. 1 (2024)
http://www.veterinaria.org
Article Received: 5th May 2024, Revised: 10th June 2024, Accepted: 4th July 2024

a typical commercial diet. SiNPs were added to Group 2 (the IC50 concentration against *Vibrio harveyi*, (i.e. 32 µg/mL): at a level of 32 ppm (1X MIC), Group 3 (2X MIC) at a dosage of 64 ppm, and Group 4 (5X MIC) at a level of 160 ppm. SiNPs were introduced to Group 5 (10X MIC) at a concentration of 320 ppm. The therapies were given to each of the experimental groups for 96 hours. The shrimps in every group were inspected throughout the trial.

2.9 CONTROL OF VIBRIOSIS INFECTION CAUSED BY *V. HARVEYI* USING SINPS *IN VIVO* MODEL

In vivo control ability of the SiNPs obtained from plant extract against *V. Harveyi* obtained from infected shrimp was determined as per the method outlined by modifications (Sakthivel, 2023). *In vivo* infectivity was developed using the method proposed by Roque *et al.,* (1998). Briefly, five marine shrimp juveniles each (9.89 ± 0.47 cm length and 3.756 ± 0.447 g weight) were acclimatized in 10 L HDPE drum containing 6 L of aged-seawater (~30 ppt). One day after acclimatization, the shrimps were individually netted out and a small wound was made using a sterile scalpel on the third abdominal segment (~ 2 mm long). The luminescent bacterial cells were grown in 250 mL Erlen Mayer flasks containing 150 mL TSA (1% NaCl). The bacterial cells were obtained after centrifugation at 4000 rpm as pellets and mixed with sterile seawater, transferred to the jar having shrimp that wounded for the analysis. The commercially available shrimp feed (Gargil, Mumbai, India) was fed with ad libitum and aeration was provided continuously. The infected shrimps were divided into four treatment groups, each set up in duplicate along with a control group. The groups were as follows: Group 1 consisted of wounded shrimp, Group 2 included wounded shrimp infected with Vibrio harveyi, Group 3 comprised wounded shrimp infected with Vibrio harveyi and treated with silver nanoparticles (SiNPs) at a concentration of 30 ppm, and Group 4 consisted of wounded shrimp infected with Vibrio harveyi and treated with streptomycin at a concentration of 30 ppm.

The presumptive Vibrio count (PVC) was estimated in the TCBS medium. About 25% of the water in each treatment was replaced with filtered seawater containing an equal concentration of SiNPs and Streptomycin as on day 1. The mortality percentage and relative percentage survival and the bacterial count were examined for 4 days (Janarthanam *et al.,* 2012).

$$\text{Mortality \%} = \frac{\text{No. of dead or infected shrimp – dead shrimp on day one}}{\text{Total no. of inoculated shrimp – dead shrimp on day one}} \times 100$$

Based on the mortality percentage, the relative percentage survival (RPS) of SiNPs shrimp was evaluated.

$$\text{RPS} = 1 - \frac{\text{Percentage of mortality treated}}{\text{Percentage of mortality control}} \times 100$$

3.0 Quantitative RT-PCR for LUX R gene expression :

3.1 RNA Extraction

RNA extraction was performed using the RNeasy Minikit (QIAGEN) as per the manufacturer's protocol. A nanodrop spectrophotometer set to 280 nm was used to measure the concentration of the separated RNA samples.

3.2. Quantitative RT-PCR for gene expression and determination of fold change value:

LuxR gene expression pattern analysis was conducted utilizing isolated RNA samples. The One Step Prime Script IIIRT-qPCR Kit was employed for quantitative real-time polymerase chain reaction (qPCR), enabling the accurate measurement of gene expression.The average fold change value was then calculated based on the CT values, representing the relative change in LuxR gene expression compared to a control condition. This analysis provides valuable insights into the regulatory mechanisms governing LuxR gene expression and allows for the identification of factors influencing its transcriptional activity. Overall, qPCR-based gene expression analysis serves as a powerful tool for studying the dynamics of gene regulation and understanding the molecular mechanisms underlying biological processes.

3.3 RESULTS AND DISCUSSION

3.4 Green synthesis Silver nanoparticle

The shade of silver nanoparticles of fluid concentrate of *Tinospora cordifolia* throughout some stretch of time changed from light green tone to light brown then to dark brown colour. The biochemical process occurred was explained as the decrease of Ag+ into Ag0. A noticeable shift in hue from dark brown to reddish brown suggested the presence of silver nanoparticles. Synthesized Silver nanoparticles was Confirmed using tool UV spectrophotometer, FTIR analyses for

REDVET - Revista electrónica de Veterinaria - ISSN 1695-7504
Vol 25, No. 1 (2024)
http://www.veterinaria.org
Article Received: 5th May 2024, Revised: 10th June 2024, Accepted: 4th July 2024

chemical compound identification and the morphological identification of size and shape of the nanoparticle was done using SEM, XRD.

3.5 UV–VIS Spectroscopy Analysis for Characterization of Synthesized Silver Nanoparticles

The UV visible spectrum was utilized to observe the stability and production of AgNPs and was the primary method of characterizing the generated nanoparticles (Fig. 1). The wavelength range covered by the spectrophotometer measurements spans from 200 to 800 nanometers (nm), encompassing both the visible and ultraviolet sections of the electromagnetic spectrum. The synthesized silver nanoparticles were monitored with the peak value of 420 nm. The peak represents the resonance frequency where the silver nanoparticles most effectively absorb light, suggesting the existence of AgNPs in the sample. The development and growth of the nanoparticles over time may be ascertained by monitoring the peak value during the synthesis process.

3.6 SEM Analysis

SEM offers important insights into the size, shape, and surface morphology of silver nanoparticles (AgNPs) that are generated from *Tinospora cordifolia*. A concentrated electron beam scans the sample's surface during SEM examination, producing high-resolution pictures that highlight the topographical characteristics of the nanoparticles. In the case of AgNPs synthesized from *T.cordifolia*, SEM analysis revealed that the nanoparticles exhibited a range of sizes, typically falling within the diameter range of 30 to 50 nanometers (nm). This variation in nanoparticle size indicates the effectiveness of the synthesis process in producing a heterogeneous population of nanoparticles (Fig. 2). As previously observed, the inclusion of various capping agents in the leaf extracts is the cause of the size variance (Song and Kim 2009). The ability to measure and observe nanoparticles at such a fine scale is essential for understanding their physical properties and behavior.

3.7 TEM Analysis

TEM pictures give complementary information to SEM in the confirmation of the size and shape of silver nanoparticles (AgNPs), providing in-depth insights into each individual nanoparticle In the case of AgNPs synthesized from *Tinospora cordifolia*, TEM micrographs confirmed the spherical form of the nanoparticles, consistent with SEM observations. Additionally, TEM analysis confirmed that the nanoparticles exhibited a size range of 30 to 50 nanometers (nm), aligning closely with the measurements obtained from SEM analysis (Fig. 3). The TEM images' validation of the produced AgNPs' spherical form and size consistency reinforces their characterisation even further. To visualize individual nanoparticles at such a fine scale provides conclusive evidence regarding their structural properties.

3.8 FTIR Analysis

The synthesized silver nanoparticle biomolecules were confirmed using the FTIR spectral measurements. Functional group presence in the biomolecules and their interactions with AgNPs are determined using FTIR spectroscopy, which measures the sample's absorption of infrared light. The different absorption of peak values obtained shows the presence of different functional groups of potential silver nanoparticles (Fig. 4). During FTIR spectral measurements, different absorption peak values are observed, indicating the presence of various functional groups associated with biomolecules like Alkyl C–H, C=O group of amides, C–F of alkyl halides, and C–O of alcohol groups. The existence of these functional groups on the AgNPs' surface suggests that the biomolecules were involved in the creation and stability of the nanoparticles.

3.9 XRD ANALYSIS

X-ray diffraction analysis (XRD) is a technique used to detect the crystal structure of materials by analyzing the diffraction pattern. When XRD was used to further analyze the biosynthesized AgNPs, it was found that the diffraction peaks had a range of 2Ɵ (10–90), which corresponded to the (2 6 4) (1 1 1) (2 0 0) plane (Figure 5). The XRD pattern was obtained over a range of 2θ angles from 10° to 90°. This range covers a significant portion of the diffraction pattern, indicating the presence of crystalline material.

REDVET - Revista electrónica de Veterinaria - ISSN 1695-7504
Vol 25, No. 1 (2024)
http://www.veterinaria.org
Article Received: 5th May 2024, Revised: 10th June 2024, Accepted: 4th July 2024

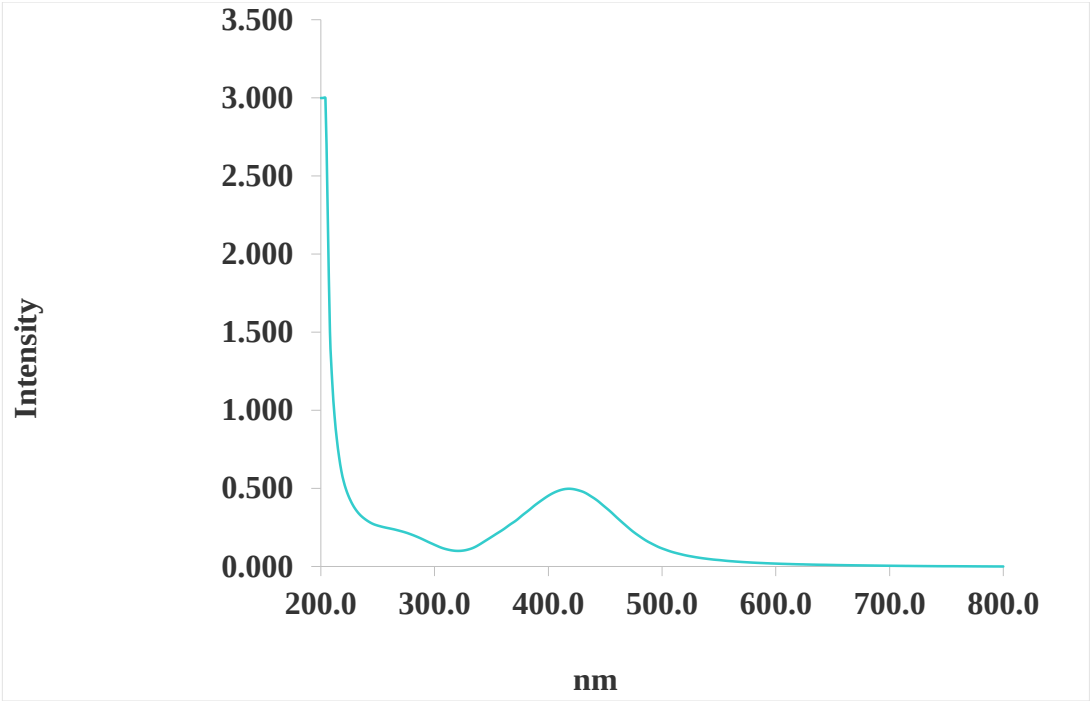

Fig. 1. Uv-vis spectroscopy analysis of silver nanoparticles

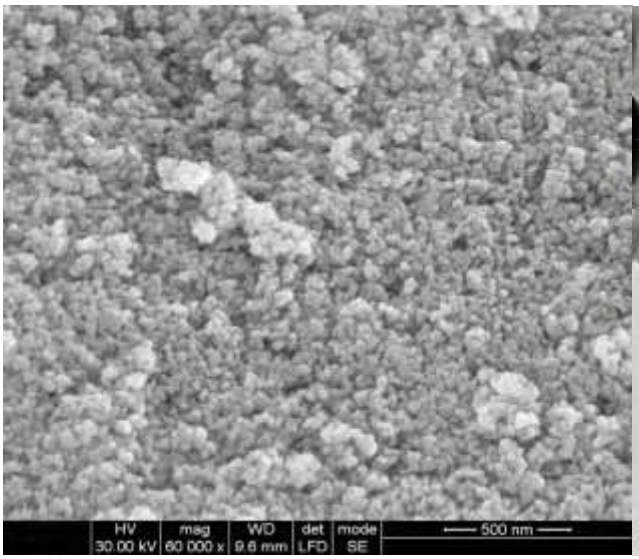

Fig.2. SEM analysis

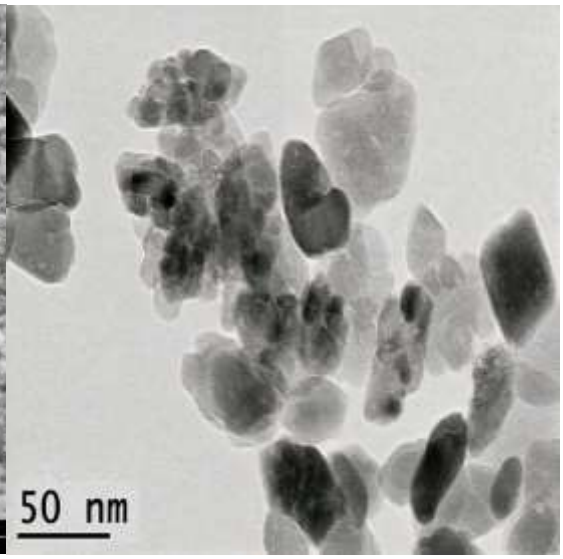

Fig.3. TEM analysis

REDVET - Revista electrónica de Veterinaria - ISSN 1695-7504
Vol 25, No. 1 (2024)
http://www.veterinaria.org
Article Received: 5th May 2024, Revised: 10th June 2024, Accepted: 4th July 2024

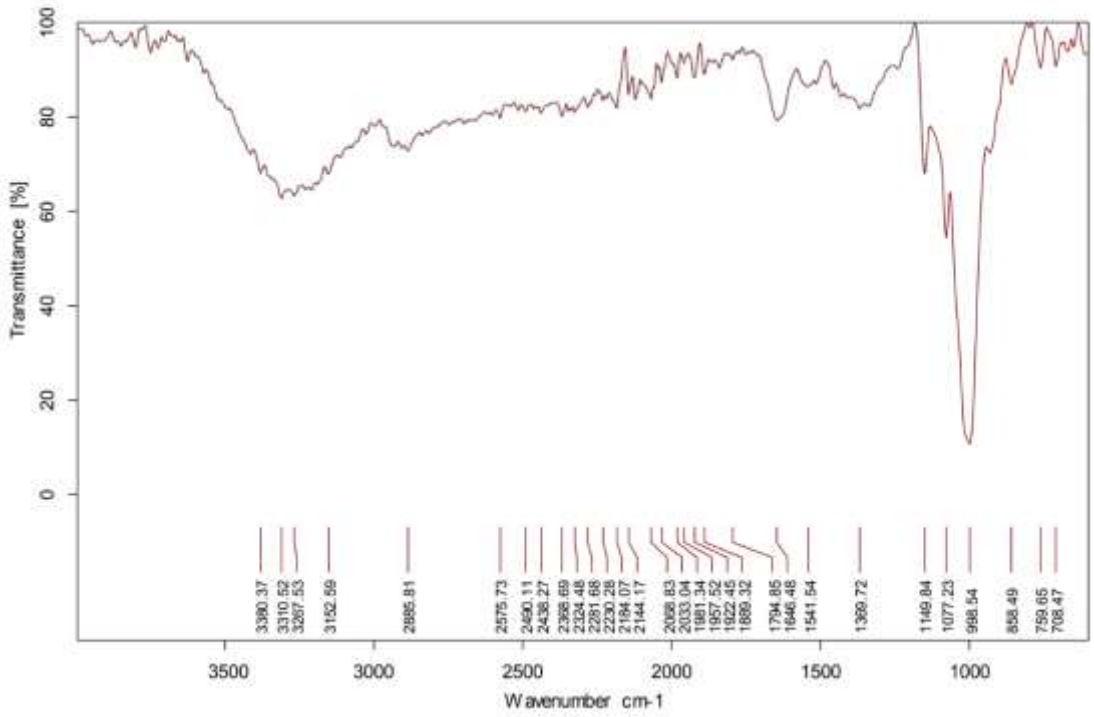

Fig. 4. FTIR analysis of synthesized silver nanoparticles

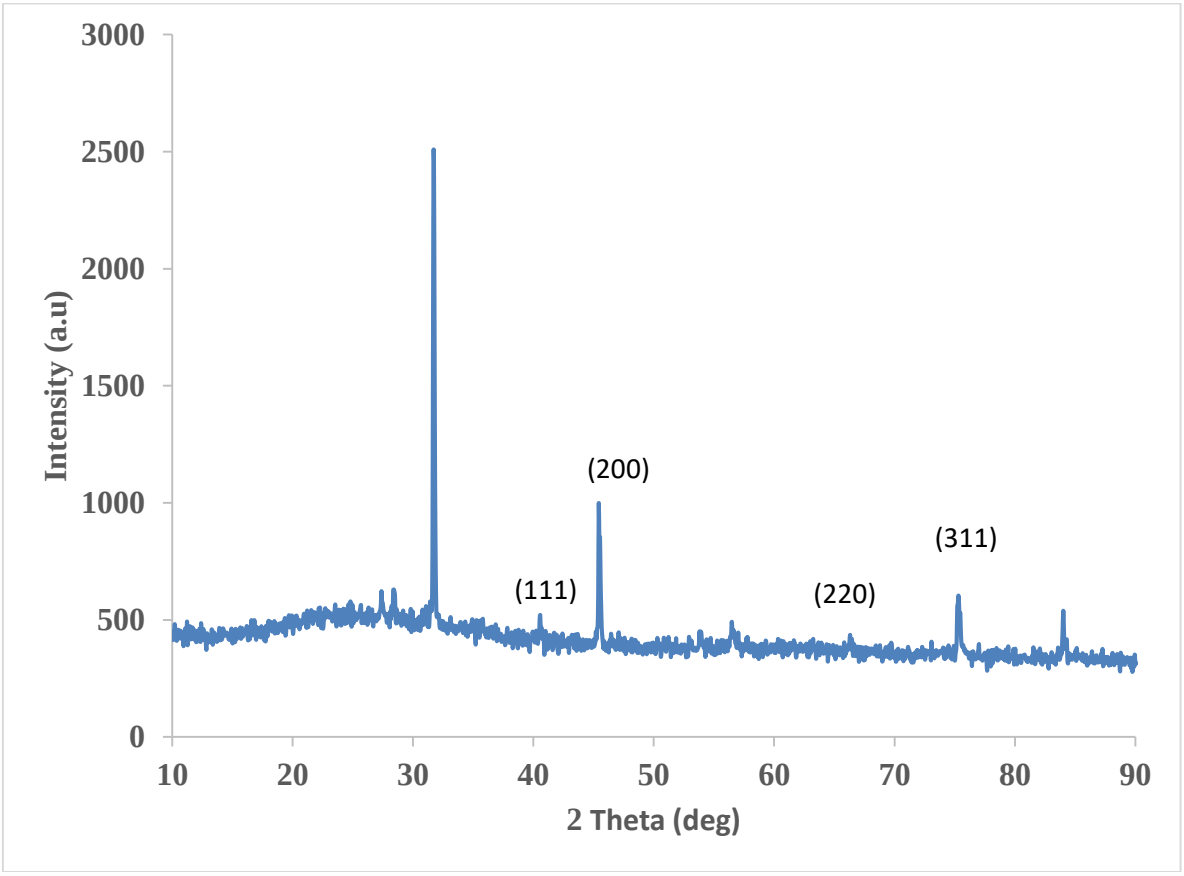

Fig. 5. XRD analysis of synthesized silver nanoparticles

REDVET - Revista electrónica de Veterinaria - ISSN 1695-7504
Vol 25, No. 1 (2024)
http://www.veterinaria.org
Article Received: 5th May 2024, Revised: 10th June 2024, Accepted: 4th July 2024

4.0 ANTIOXIDANT STUDIES

Antioxidant activity was determined using ABTS, FRAP, DPPH and Nitric oxide (NO) assay. It was performed using the silver nanoparticles of the *Tinospora cordifolia* plant extract and the maximum activity and minimum activity was measured at different sample concentration with optical density.

4.1.1 ABTS assay

Radial scavenging activity of sample using ABTS assay. It was performed using the silver nanoparticles of the *Tinospora cordifolia* plant extract, it showed maximum activity at 36.18 % at 0.4(µM) sample concentration with optical density of 0.448 and minimum activity shown at 15.95 % at 0.1 (µM) sample concentration.with optical density of 0.59. The radial scavenging activity of silver nanoparticles synthesized from *Tinospora cordifolia* plant extract was assessed using the ABTS assay, a widely employed method to evaluate antioxidant potential. The results indicated varying degrees of antioxidant activity depending on the concentration of the sample. At a concentration of 0.4 µM, the silver nanoparticles exhibited their highest activity, demonstrating a substantial 36.18% inhibition of ABTS radicals. This indicates a strong ability to neutralize free radicals, which are implicated in oxidative stress and various diseases (Table 1).

4.1.2 FRAP assay

Determination of antioxidant activity using FRAP (Ferric Reducing Antioxidant Power) assay. The FRAP assay was done according to (Benzie and Strain., 1999) with some modifications. it showed maximum activity at 40.31% a t 0.1 (µM) sample concentration with optical density of 0.345 and minimum activity shown at 1.21 % at 0.5 (µM) sample concentration.with optical density of 0.571. At a concentration of 0.1 µM, the silver nanoparticles demonstrated their highest activity, exhibiting a substantial 40.31% reduction in ferric ions. This suggests a potent ability to donate electrons and neutralize free radicals, consistent with strong antioxidant properties (Table 2).

4.1.3 DPPH assay

The (1,1-diphenyl-2-picrylhydrazyl) DPPH test is used to examine antioxidant activity.. The highest inhibition activity was recorded at 54.94 % at 0.3 (µM) concentration with optical density of 0.278 and lowest activity of nanoparticle was 29.17 % at 0.3 (µM) concentration with optical density 0.437. The corresponding optical density at this concentration was measured at 0.278, suggesting a relatively low absorbance of light due to the effective scavenging of DPPH radicals by the nanoparticles (Table 3).

4.1.4 NO Assay

The Griess reaction was used to quantify the nitric oxide produced when sodium nitroprusside was added to an aqueous solution at a physiological pH (Marcocci *et al*., 1994). Nitric acid scavenging ability of Silver nanoparticle maximum inhibition was 26.37 % at 0.2 (µM) concentration with optical density 0.402 and 3.66 % at 0.5 (µM) sample concentration with optical density of 0.526. The maximum suppression of nitric oxide was achieved by the silver nanoparticles at a concentration of 0.2 µM, showing a significant 26.37% inhibition rate. The aforementioned suggests that the nanoparticles possess a noteworthy capacity to scavenge nitric oxide radicals, which are connected to several physiological processes and oxidative stress. As a result of the nanoparticles' effective scavenging of nitric oxide radicals, the optical density measured at this concentration was 0.402, indicating a comparatively low light absorption (Table 4).

Table.1. ABTS assay

SL.NO.	Sample Concentration(µM)	METHOD	Optical Density	RESULTS (% inhibition)
1	Control	ABTS assay	0.702	0.00
2	0.1		0.59	15.95
3	0.2		0.557	20.66
4	0.3		0.483	31.20
5	0.4		0.448	36.18
6	0.5		0.523	25.50

Table.2. FRAP assay

SL.NO.	Sample Concentration(µM)	METHOD	Optical Density	RESULTS (% inhibition)
1	Control		0.578	0.00
2	0.1		0.345	40.31

REDVET - Revista electrónica de Veterinaria - ISSN 1695-7504
Vol 25, No. 1 (2024)
http://www.veterinaria.org
Article Received: 5th May 2024, Revised: 10th June 2024, Accepted: 4th July 2024

3	0.2	FRAP assay	0.408	29.41
4	0.3		0.523	9.52
5	0.4		0.54	6.57
6	0.5		0.571	1.21

Table.3. DPPH assay

SL.NO.	Sample Concentration (µM)	METHOD	Optical Density	RESULTS (% inhibition)
1	Control	DPPH assay	0.617	0.00
2	0.1		0.437	29.17
3	0.2		0.34	44.89
4	0.3		0.278	54.94
5	0.4		0.319	48.30
6	0.5		0.436	29.34

Table.4. NO assay

SL.NO.	Sample Concentration (µM)	METHOD	Optical Density	RESULTS (% inhibition)
1	Control	NO assay	0.546	0.00
2	0.1		0.435	20.33
3	0.2		0.402	26.37
4	0.3		0.469	14.10
5	0.4		0.511	6.41
6	0.5		0.526	3.66

4.2 Antibacterial Activity

Antimicrobial activity of silver nanoparticles synthesized from *Tinospora cordifolia* plant extract against the bacteria are *Staphylococcus aureus*, *Pseudomonas aeruginosa*, *Salmonella typhi* and *V.harveyi* was investigated and the diameter of zone of inhibition in triplicate plates was calculated. Maximum inhibition was noted in *Vibrio Harveyi* (33 mm in 100 µg/mL),*Pseudomonas aeruginosa* (34 mm in 100 µg/mL), *Salmonella typhi* (17 mm in 100 µg/mL), *Staphylococcus aureus* (33 mm in 100 µg/mL).The results revealed varying degrees of inhibition against the different bacterial strains. Notably, the maximum inhibition was observed against *Vibrio harveyi* and *Pseudomonas aeruginosa*, with zone diameters of 33 mm and 34 mm.These findings underscore the broad-spectrum antimicrobial efficacy of the silver nanoparticles, as they demonstrated significant inhibitory effects against both Gram-positive (*Staphylococcus aureus*) and Gram-negative (*Pseudomonas aeruginosa*, *Salmonella typhi*, *V.harveyi*) bacterial strains. The observed variation in the zone of inhibition values among different bacterial strains suggests that the antimicrobial activity of the silver nanoparticles may be influenced by the specific phytochemical composition of the *Tinospora cordifolia* plant extract used for their synthesis (Table 5).

Table.5.Antibacterial activity of various test samples

Name of the Sample	ZOI(mm)					ZOI (mm) Standard*
	0 µg/mL	25 µg/mL	50 µg/mL	75 µg/mL	100 µg/mL	30µg/well
Pseudomonas aeruginosa	-	31	32	33	34	10
Salmonella typhi	-	14	15	16	17	22
Staphylococcus aureus	-	29	30	31	33	14
Vibrio harveyi	-	28	29	31	33	28

REDVET - Revista electrónica de Veterinaria - ISSN 1695-7504
Vol 25, No. 1 (2024)
http://www.veterinaria.org
Article Received: 5th May 2024, Revised: 10th June 2024, Accepted: 4th July 2024

4.3 LC 50

The LC50 of SiNPs was determined using *L. vannamei* on aquarium model. The results evident that up to 5X MIC concentrations did not kill the animal up to 96 h (Table 1). In the 10X MIC concentration showed mortality of 20% at 48 h and 72 h and 40% was attained at 96 h. While the 96 h LC50 value (with 95% confidence limits) of the safe dose of SiNPs was estimated at LC50=396.6 ppm. The morphology of the animal did not show any variations between the groups (Table 6).

Table.6. LC50 of synthesized silver nanoparticles

Concentrations (ppm)	Mortality (%)				
	0h	24h	48h	72h	96h
Group 1 (0 ppm)	0	0	0	0	0
Group 2 (1X MIC i.e. 32 ppm)	0	0	0	0	0
Group 3 (2X MIC i.e. 64 ppm)	0	0	0	0	0
Group 4 (5X MIC i.e. 160 ppm)	0	0	0	0	0
Group 5 (10X MIC i.e. 320 ppm)	0	0	20	20	40

4.4 CONTROL OF VIBRIOSIS INFECTION CAUSED BY *V. HARVEYI* USING SiNPs *IN VIVO* MODEL

In vivo, the disease control activity of SiNPs against luminescent vibriosis causing pathogenic *V. harveyi* was determined by the aquarium method. The disease control potential of the SiNPs against *V. harveyi* was remarkable and able to control it underwater and reduce the pathogenicity on artificially wounded shrimp (Figures 6A, 6B). The mortality percentage on a daily basis up to 4 days after inoculation showed a significant disease protection effect of SiNPs (Fig.7). The RPS values of the challenged shrimp on the 4th day of the challenge were 85.71% for both SiNPs and antibiotics treatments, respectively (Fig.8).The presumptive vibrio load (Fig.9) had little variation during the experimental period. The detailed spectrum of the bacterial population during the challenge study results is described in Table 7. Presumptive Vibrio count was reduced more in SiNPs and antibiotic treatment. Among the tested treatments, the SiNPs and antibiotics treatments showed a very good disease reduction in terms of lesser vibrio count and mortality perncentage and higher RPS.

Table 7: *In vivo* antibacterial activity of SiNPs against *V. harveyi* was challenged with *L. vannamei*

Presumptive Vibrio Count				
Treatments	**Day.1**	**Day.2**	**Day.3**	**Day.4**
Vibrio Control	1.71×10^{7}	1.16×10^{8}	1.56×10^{9}	1.89×10^{9}
SiNPs	3.5×10^{5}	2.6×10^{3}	8.2×10^{2}	1.3×10^{2}
Streptomycin	1.42×10^{5}	1.32×10^{3}	5.8×10^{2}	1.1×10^{2}

Control under White Light **Control Under UV**

REDVET - Revista electrónica de Veterinaria - ISSN 1695-7504
Vol 25, No. 1 (2024)
http://www.veterinaria.org
Article Received: 5th May 2024, Revised: 10th June 2024, Accepted: 4th July 2024

Disease Control White Light **Disease Control under UV**

Fig.6A. Effect of SiNPs on the control of luminescent vibriosis in vivo model

SiNPs under White Light **SiNPs under UV**

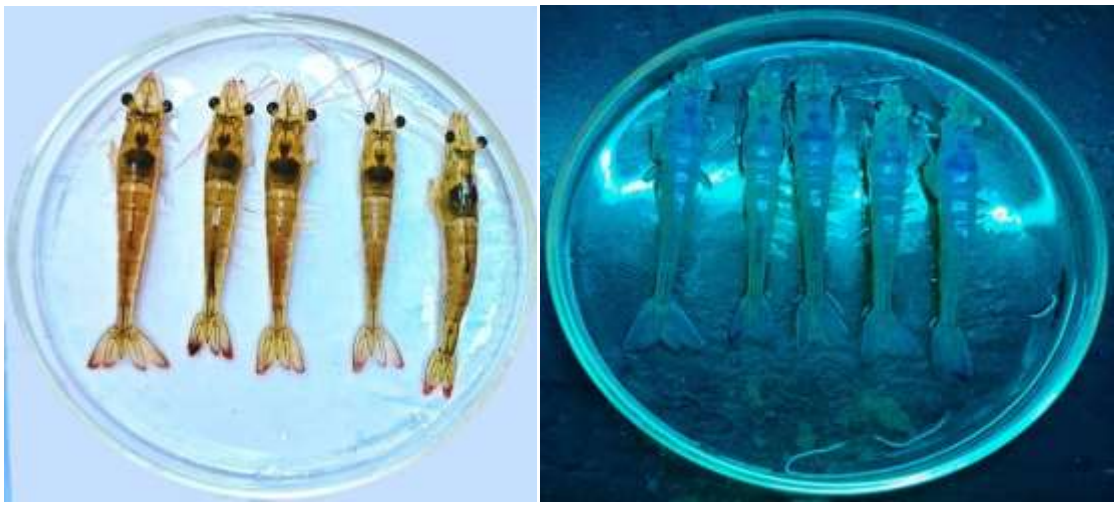

Disease Control White Light **Disease Control under UV**

REDVET - Revista electrónica de Veterinaria - ISSN 1695-7504
Vol 25, No. 1 (2024)
http://www.veterinaria.org
Article Received: 5th May 2024, Revised: 10th June 2024, Accepted: 4th July 2024

Fig.6B. Effect of SiNPs on the control of luminescent vibriosis in vivo model

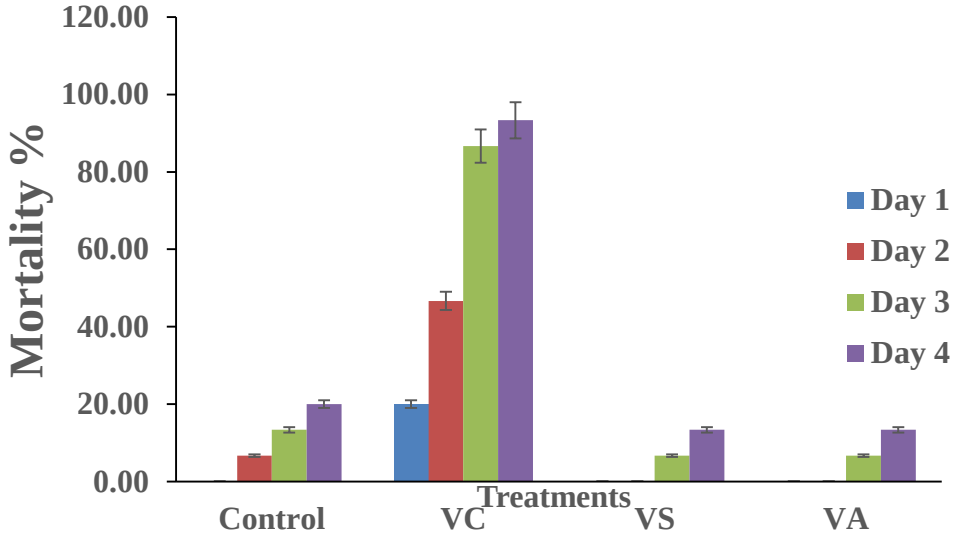

Fig.7. Mortality rate of SiNPs on the control of luminescent vibriosis on *L. vannamei* in vivo model

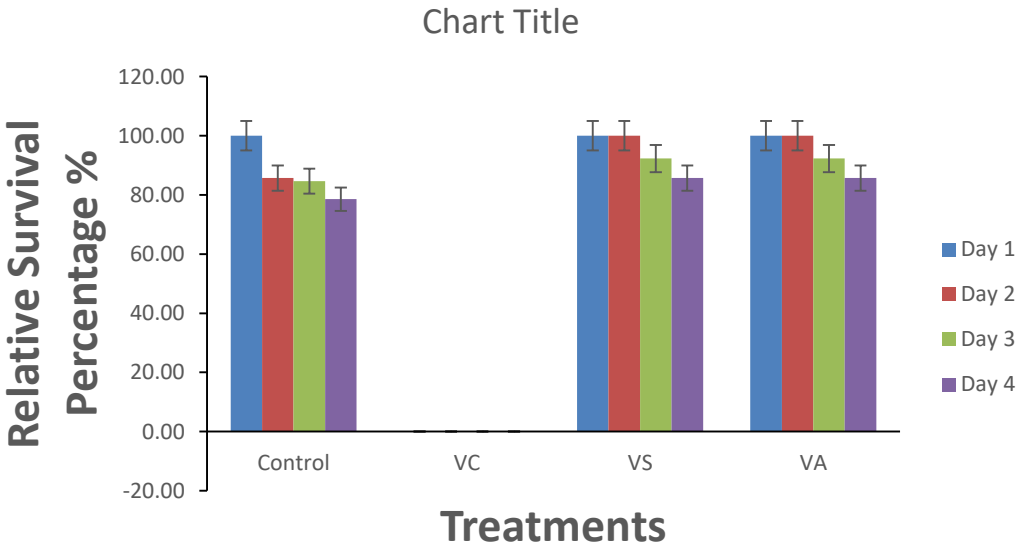

Fig.8. Relative survival percentage of SiNPs on the control of luminescent vibriosis on *L. vannamei* in vivo model

REDVET - Revista electrónica de Veterinaria - ISSN 1695-7504
Vol 25, No. 1 (2024)
http://www.veterinaria.org
Article Received: 5th May 2024, Revised: 10th June 2024, Accepted: 4th July 2024

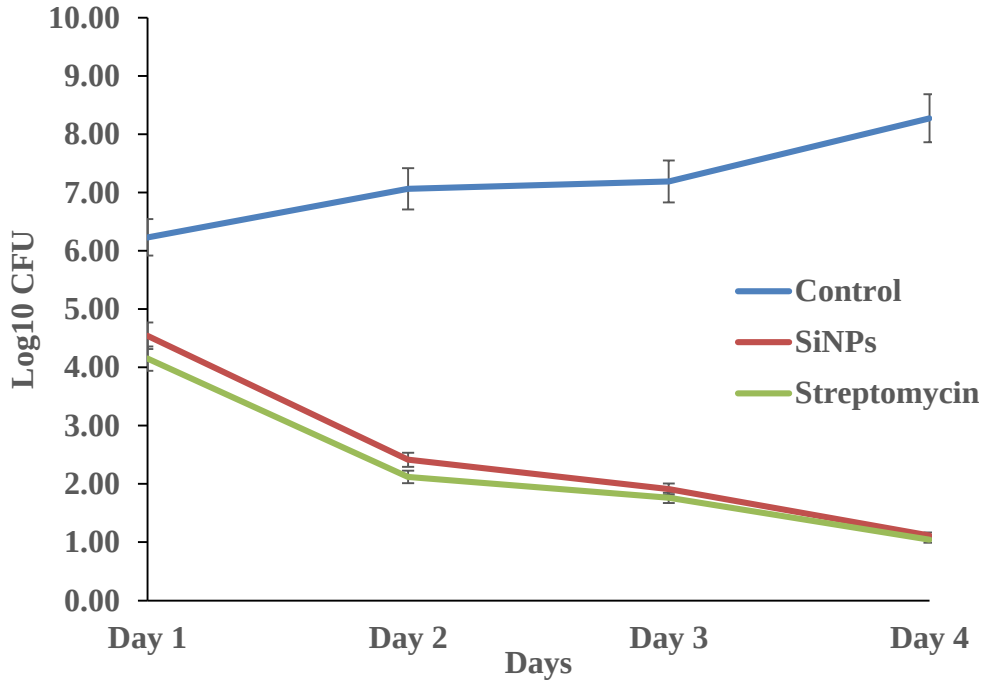

Fig.9. Presumptive vibrio count of SiNPs on the control of luminescent vibriosis on *L. vannamei* in vivo model

4.5 RNA extraction

RNA extraction was performed using the QIAGEN RNeasy Minikit and the manufacturer's instructions were followed exactly. A Nanodrop spectrophotometer calibrated to 280 nm was used to quantify the concentration of the extracted RNA samples. Since this wavelength matches the absorbance peak of RNA, it is frequently used to quantify nucleic acids, including RNA. The quantity of RNA in the sample may be ascertained by measuring the absorbance at this particular wavelength, which provides important information for subsequent processes like cDNA synthesis and gene expression analysis.

Table.8.Concentration of the isolated RNA samples

Sample ID	Concentration (µg/ml)	**280/260**
Control	106.8	1.80
Treated	128.9	1.82

4.5.1 Quantitative RT-PCR for gene expression:

Gene expression pattern analysis was performed using the isolated RNA sample and One Step prime Script iiiRT-qPC RKit (TAKARA) by following the parameters and respective gene-specific primers. Starting at 42°C for 60 minutes, complementary DNA synthesis (cDNA synthesis) was performed to convert RNA to complementary DNA. After that, to deactivate the enzymes and guarantee the integrity of the ensuing processes, heat inactivation was performed for ten minutes at 70°C. In order to ensure that the enzyme was activated and the DNA strands were separated, the process for amplification of the target DNA initiated with an initial denaturation and Hot start Taq activation phase at 95°C for 10 minutes. The amplification cycle then consists of 35 cycles, with each cycle including 15 seconds of denaturation at 95°C, 15 seconds of annealing at 60°C, and 15 seconds of extension at 60°C.The identifications of the target sequences was made possible by detecting the amplified DNA at 60°C for 15 seconds after the amplification cycles. Lastly, a melting curve analysis was carried out between 40°C and 95°C in order to evaluate the amplified products' specificity and identify any instances of primer-dimer formation or non-specific amplification. This multi-phase procedure allows for accurate and fast target DNA sequence amplification and detection at each step, all while requiring perfect temperature control.

4.5.2 Melting curve analysis

Table.9.Gene:-LuxR

Sample ID	Ct	**Melting curve temperature**
Control	29.0	73.7

REDVET - Revista electrónica de Veterinaria - ISSN 1695-7504
Vol 25, No. 1 (2024)
http://www.veterinaria.org
Article Received: 5th May 2024, Revised: 10th June 2024, Accepted: 4th July 2024

Treated	23.3	73.5

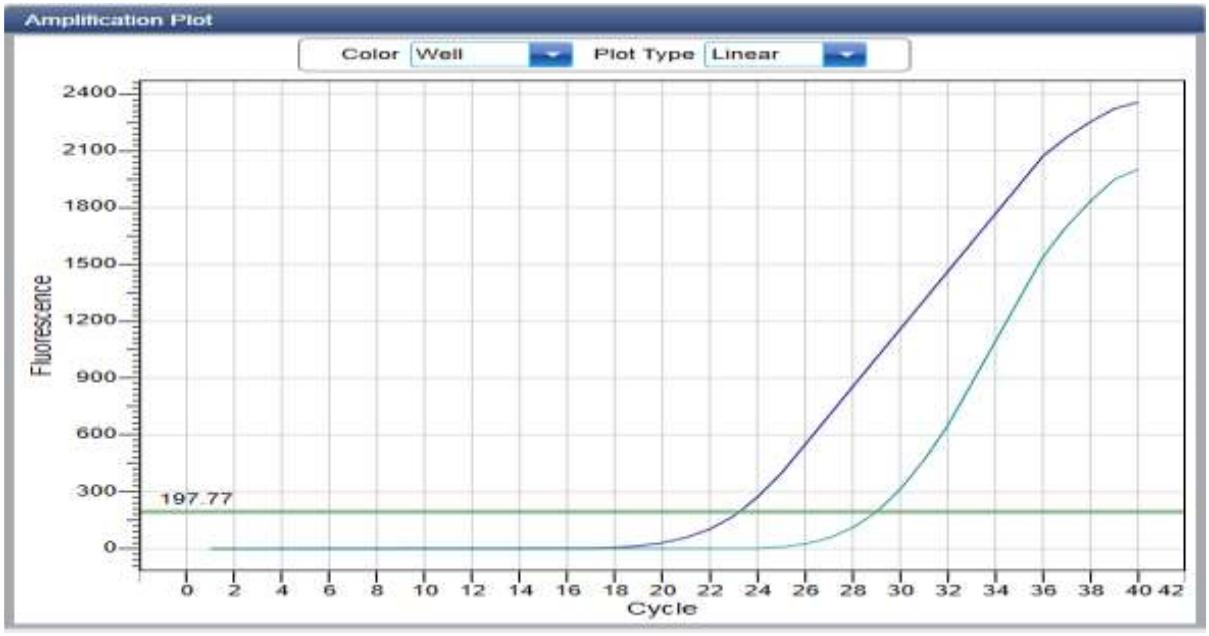

Fig.10.The amplification plot for sample Control and treated LuxR gene

Table.10. Gene :- 16S RNA

Sample ID	Ct	**Melting curve temperature**
Control	29.6	78.4
Treated	22.7	78,5

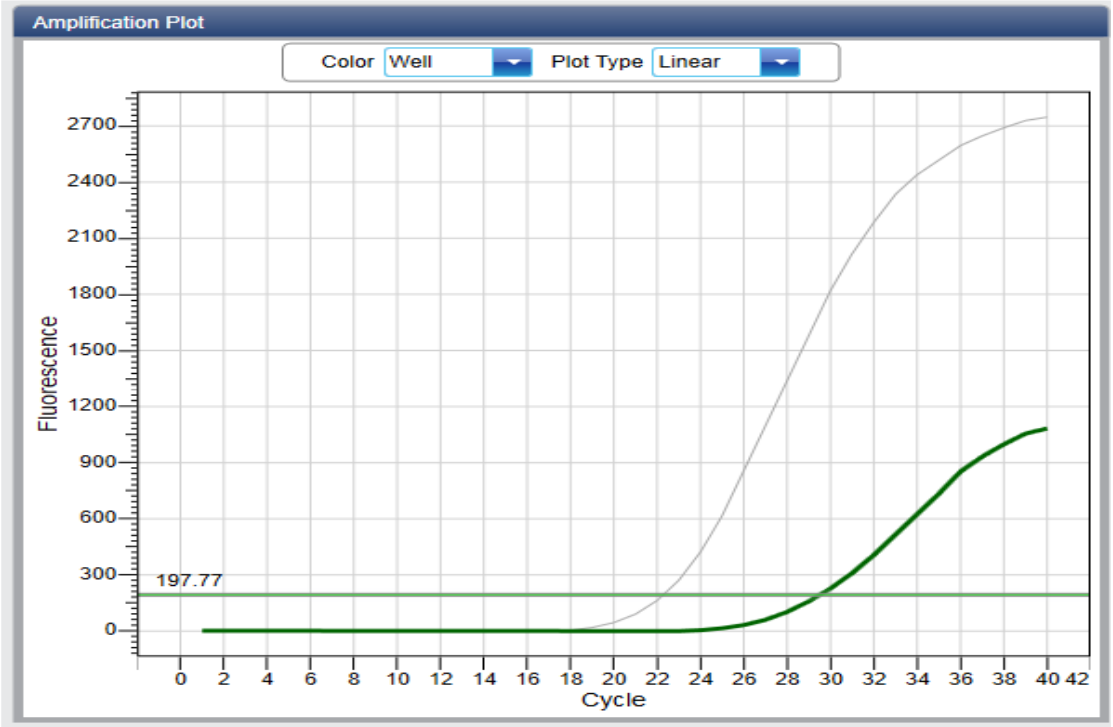

Fig.11.The amplification plot for sample Control and treated 16s rRNA

4.6 Determination of fold change value:

Gene expression pattern analysis was conducted by isolating RNA samples and calculating fold change values to assess the expression of the LuxR gene. Fold change, indicative of variation in quantity between initial and subsequent

REDVET - Revista electrónica de Veterinaria - ISSN 1695-7504
Vol 25, No. 1 (2024)
http://www.veterinaria.org
Article Received: 5th May 2024, Revised: 10th June 2024, Accepted: 4th July 2024

measurements, serves as a vital metric in gene expression data analysis. Specifically, the average fold change values for both control and treated samples were determined. In Table.11, it was observed that the fold change values decreased after treatment. This reduction from an initial average fold change value of 1.11±0.18 to 0.56±0.11 indicated a decrease in gene expression. The calculation of fold change values relied on CT (threshold cycle) values, a common method in gene expression analysis. The decrease in fold change values post-treatment signified a downregulation in LuxR gene expression, suggesting a potential impact of the treatment on gene regulation within the studied biological system.

Table.11. Calculation of Fold change using Ct Values.

Treatments	16SrRNA			LUX gene			CT and Fold Change			
	CT 1	CT 2	Average CT	CT 1	CT 2	AVG CT	Δ CT	ΔΔCT	Fold Change	Average Fold Change + Standard Deviation
Control	29.6	29.2	29.4	29.3	29	29.15	0.25	0.03	0.98	**1.11±0.18**
Control	29.5	29.4	29.45	29.2	29.1	29.15	0.3	-0.30	1.23	
Treated	22.7	22.9	22.8	23.3	23.6	23.45	-0.65	0.65	0.64	**0.56±0.11**
Treated	22.6	22.5	22.55	23.5	23.7	23.6	-1.05	1.05	0.48	

5. CONCLUSION

The synthesis of silver nanoparticles using *Tinospora cordifolia* presents a promising avenue for several reasons. Firstly, the process is cost-effective, making it economically feasible for large-scale production. *Tinospora cordifolia*, commonly known as Giloy, is a readily available medicinal plant, which makes it a sustainable source for nanoparticle synthesis. This aspect is crucial for industries aiming to adopt environmentally friendly practices. Moreover, the synthesized nanoparticles demonstrated reliability in terms of their efficacy as therapeutic agents. The RT-PCR examination revealed a decrease in the fold change value, indicating a downregulation of gene expression. This finding suggests that the nanoparticles may have a regulatory effect on the genetic mechanisms associated with bacterial infections, potentially inhibiting their proliferation or virulence.

Furthermore, the nanoparticles exhibited notable antioxidant and antibacterial properties against vibriosis infection in shrimp. By effectively combating bacterial infection, the *Tinospora cordifolia* silver nanoparticles offer a promising alternative to conventional chemical medications. Unlike some chemical treatments which may lead to the development of resistance in bacteria or cause adverse effects, these nanoparticles appear to be a safer and more sustainable option. Additionally, exploring the bioactivity of easily accessible herbs like *Tinospora cordifolia* opens up avenues for the development of novel therapeutic strategies. This approach not only enhances our understanding of traditional medicinal plants but also offers opportunities for innovation in healthcare. Continued research and exploration in this area are likely to yield further insights and applications, contributing to the development of sustainable and effective solutions for healthcare and aquaculture.

4.7 COMPETING INTERESTS

Authors have declared that no competing interests exist.

4.8 REFRENCES

1. Ahmadi, S., Askani, S., Fathima, S., Bushra, M., Sumayya, P. S., Charan, J. P., ... & Taduri, S. (2023). Preliminary phytochemical screening and antibacterial activity of Tinospora cordifolia.
2. Babu, B., Sathiyaraj, G., Mandal, A., Kandan, S., Biju, N., Palanisamy, S., ... & Prabhu, N. M. (2021). Surveillance of disease incidence in shrimp farms located in the east coastal region of India and in vitro antibacterial efficacy of probiotics against Vibrio parahaemolyticus. *Journal of invertebrate pathology*, *179*, 107536.
3. Benzie, I. F. and Strain, J. J. (1999). [2] Ferric reducing/antioxidant power assay: direct measure of total antioxidant activity of biological fluids and modified version for simultaneous measurement of total antioxidant power and ascorbic acid concentration. In *Methods in enzymology (Vol. 299, pp. 15-27).* Academic press.
4. Dar, W. (1999, March). Sustainable aquaculture development and the code of conduct for responsible fisheries. In *The Ministerial Meeting on the Implementation of the Code of Conduct for Responsible Fisheries. Rome*.
5. De La Pena, L. D., Lavilla-Pitogo, C. R. and Paner, M. G. (2001). Luminescent vibrios associated with mortality in pond-cultured shrimp Penaeus monodon in the Philippines: species composition. *Fish Pathology*, *36*(3), 133-138.

6. Dhar, A. K., Piamsomboon, P., Caro, L. F. A., Kanrar, S., Adami Jr, R. and Juan, Y. S. (2019). First report of acute hepatopancreatic necrosis disease (AHPND) occurring in the USA. *Diseases of aquatic organisms*, *132*(3), 241-247.
7. FAO, (2020). The State of World Fisheries and Aquaculture 2020. Sustainability in action, Rome. https://doi.org/10.4060/ca9229en (accessed on 22nd July 2020).
8. (FAO, (2016). The State of World Fisheries and Aquaculture 2016. Contributing to food security and nutrition for all. Rome. pp. 200.
9. Gulec, A. K., AltİnterİM, B. A. Ş. A. R. and Aksu, O. (2013). Determination of lethal concentration (LC50) values of Cinnamomum zeylanicum hydrosol on carp fish. *Iranian Journal of Fisheries Sciences*, *12*(1), 34-44.
10. Holder, I. A. and Boyce, S. T. (1994). Agar well diffusion assay testing of bacterial susceptibility to various antimicrobials in concentrations non-toxic for human cells in culture. *Burns*, *20*(5), 426-429.
11. Inglis, V. (2000). Antibacterial chemotherapy in aquaculture: review of practice, associated risks and need for action. In *Use of Chemicals in Aquaculture in Asia: Proceedings of the Meeting on the Use of Chemicals in Aquaculture in Asia 20-22 May 1996, Tigbauan, Iloilo, Philippines* (pp. 7-22). Aquaculture Department, Southeast Asian Fisheries Development Center.
12. Iswarya, A., Marudhupandi, T., Vaseeharan, B., Ibrahim, W. N. W., Leong, L. K., & Musa, N. (2022). Shrimp vibriosis. In *Aquaculture pathophysiology* (pp. 191-206). Academic Press.
13. Janarthanam, K., George, M. R., John, K. R. and Jeyaseelan, M. J. (2012). *In vitro* and *in vivo* biocontrol of *Vibrio harveyi* using indigenous bacterium, *Bacillus spp*.
14. Li, P., Kinch, L. N., Ray, A., Dalia, A. B., Cong, Q., Nunan, L. M. and Orth, K. (2017). Acute hepatopancreatic necrosis disease-causing Vibrio parahaemolyticus strains maintain an antibacterial type VI secretion system with versatile effector repertoires. *Applied and environmental microbiology*, *83*(13), e00737-17.
15. Marcocci, L., Maguire, J. J., Droylefaix, M. T., & Packer, L. (1994). The nitric oxide-scavenging properties of Ginkgo biloba extract EGb 761. *Biochemical and biophysical research communications*, *201*(2), 748-755.
16. Modi, Bindu, Niranjan Koirala, Surya Prasad Aryal, Jiban Shrestha, Shishir Koirala, Jitendra Upadhyaya, Ram Chandra Basnyat, Mohamed A. Nassan, Mohammed Alqarni, and Gaber El-Saber Batiha. "Tinospora cordifolia (Willd.) Miers: phytochemical composition, cytotoxicity, proximate analysis and their biological activities." *Cellular and Molecular Biology* 67, no. 1 (2021): 50-57.
17. MPEDA, 2016. The Marine Product Development Authority (MPEDA) State-wise details of shrimp and scampi production. Accessed 13 February 2018. http://mpeda.gov.in.
18. Namrta Choudhary, N. C., Siddiqui, M. B., Shazia Azmat, S. A., & Sayyada Khatoon, S. K. (2013). Tinospora cordifolia: ethnobotany, phytopharmacology and phytochemistry aspects.
19. Pirtarighat, S., Ghannadnia, M. and Baghshahi, S. (2019). Green synthesis of silver nanoparticles using the plant extract of Salvia spinosa grown in vitro and their antibacterial activity assessment. *Journal of Nanostructure in Chemistry*, *9*, 1-9.
20. Re, R., Pellegrini, N., Proteggente, A., Pannala, A., Yang, M. and Rice-Evans, C. (1999). Antioxidant activity applying an improved ABTS radical cation decolorization assay. *Free radical biology and medicine*, *26*(9-10), 1231-1237..
21. Rhodes, G., Huys, G., Swings, J., Mcgann, P., Hiney, M., Smith, P., & Pickup, R. W. (2000). Distribution of oxytetracycline resistance plasmids between aeromonads in hospital and aquaculture environments: implication of Tn 1721 in dissemination of the tetracycline resistance determinant Tet A. *Applied and environmental microbiology*, *66*(9), 3883-3890.
22. Roque, A., Turnbull, J. F., Escalante, G., Gomez-Gil, B. and Alday-Sanz, M. V. (1998). Development of a bath challenge for the marine shrimp Penaeus vannamei Boone, 1931. *Aquaculture*, *169*(3-4), 283-290.
23. Saxena, C., & Rawat, G. (2019). Tinospora cordifolia (Giloy)-Therapeutic uses and importance: A review. *Current Research in Pharmaceutical Sciences*.
24. Sharma, P., Dwivedee, B. P., Bisht, D., Dash, A. K., & Kumar, D. (2019). The chemical constituents and diverse pharmacological importance of Tinospora cordifolia. *Heliyon*, *5*(9).
25. Sinha, K., Mishra, N. P., Singh, J. and Khanuja, S. P. S. (2004). *Tinospora cordifolia* (Guduchi), a reservoir plant for therapeutic applications: A Review.
26. Song, J. Y., & Kim, B. S. (2009). Rapid biological synthesis of silver nanoparticles using plant leaf extracts. *Bioprocess and biosystems engineering*, *32*, 79-84.
27. Sørum, H. (1999). Antibiotic resistance in Aquaculture. Acta Veterinaria Scandinavia, Supplementum, 92, 29–36.
28. Soto-Rodriguez, S. A., Gomez-Gil, B. and Lozano, R. (2010). 'Bright-red'syndrome in Pacific white shrimp *Litopenaeus vannamei* is caused by *Vibrio harveyi*. *Diseases of aquatic organisms*, *92*(1), 11-19.
29. Tacon, A. G. (2020). Trends in global aquaculture and aquafeed production: 2000–2017. *Reviews in Fisheries Science & Aquaculture*, *28*(1), 43-56.

30. Teng, T., Liang, L., Chen, K., Xi, B., Xie, J. and Xu, P. (2017). Isolation, identification and phenotypic and molecular characterization of pathogenic *Vibrio vulnificus* isolated from *Litopenaeus vannamei*. *PLoS One*, *12*(10), e0186135.
31. Thornber, K., Verner-Jeffreys, D., Hinchliffe, S., Rahman, M. M., Bass, D., & Tyler, C. R. (2020). Evaluating antimicrobial resistance in the global shrimp industry. *Reviews in aquaculture*, *12*(2), 966-986.
32. UDDIN, M. H., HASAN, M., AHASAN, M. M., HOSSAIN, M. A., & UDDIN, A. J. (2010). ANTIMICROBIAL AND CYTOTOXIC ACTIVITIES OF TINOSPORA CORDIFOLIA. *Int. J. Sustain. Agril. Tech*, *6*(12), 01-03.
33. Von Gadow, A., Joubert, E. and Hansmann, C. F. (1997). Comparison of the antioxidant activity of aspalathin with that of other plant phenols of rooibos tea *(Aspalathus linearis*), α-tocopherol, BHT, and BHA. *Journal of agricultural and food chemistry*, *45*(3), 632-638.
34. Wagner, H. (1999). *Immunomodulatory agents from plants*. Springer Science & Business Media.
35. Yen, G. C. and Duh, P. D. (1994). Scavenging effect of methanolic extracts of peanut hulls on free-radical and active-oxygen species. *Journal of agricultural and food chemistry*, *42*(3), 629-632.
36. Yu, C., Tang, J., Liu, X., Ren, X., Zhen, M. and Wang, L. (2019). Green biosynthesis of silver nanoparticles using *Eriobotrya japonica* (Thunb.) leaf extract for reductive catalysis. *Materials*, *12*(1), 189.